To appear in the 53rd ARFTG Digest, June 1999

DISTRIBUTED NONLINEAR EFFECTS IN PLANAR TRANSMISSION LINES*

James C. Booth, J.A. Beall, L.R. Vale, and R.H. Ono
National Institute of Standards and Technology, 325 Broadway, Boulder, CO 80303

Abstract - We present calculations of the third-order intercepts for planar transmission lines that contain a distributed nonlinear inductance or capacitance. We model such a transmission line as a series of small nonlinear elements that interact only weakly. This approach allows us to use simple lumped-element models to describe nonlinear effects in transmission lines longer than the effective wavelength. We use this approach to calculate the third-order intercepts for a lossless transmission line, and also for a transmission line with finite attenuation. Calculations for the lossless case agree well with third-harmonic measurements of high temperature superconducting transmission lines as a function of line length. For transmission lines with loss, the calculations agree well with third-harmonic measurements of transmission lines of variable length incorporating ferroelectric thin films.

I. Introduction

A number of new thin film materials such as the high T_c superconductors and ferroelectrics display significant nonlinear behavior in their response over a range of frequencies from audio through the microwave and millimeter wave. These materials are currently being developed for advanced high-speed electronics, where nonlinear effects are undesirable and can significantly degrade overall system performance. High T_c superconductor (HTS) materials are being exploited for their extremely low loss in receivers for wireless and telecommunications systems. In these applications unwanted interference signals are generated from nonlinear mixing processes. Ferroelectric materials have a dielectric constant ε_r that changes with the application of a bias field and are attractive for applications that require electronic tuning. As a result of the electric field dependence of ε_r, microwave circuits incorporating these materials also display significant nonlinear effects. To accurately predict application performance and to minimize deleterious effects, it has become increasingly important to understand the nonlinear properties of circuits incorporating one or more of these new thin film materials.

To describe the response of weakly nonlinear systems, simple lumped-element models of nonlinear components are often used. While this approach is attractive for its simplicity, the application of lumped-element models to describe circuits such as transmission lines that may be comparable to or longer than the effective wavelength is of questionable validity. On the other hand, a full analysis of a distributed nonlinear system is complicated. In this paper, we present a model for the nonlinear response of microwave transmission lines based on the lumped-element approach that is valid for lines of arbitrary lengths. The model can also describe nonlinear transmission lines that have finite attenuation. This model can be used to interpret experimental data on the nonlinear response of transmission lines fabricated from HTS and ferroelectric samples.

We study the nonlinear effects experimentally using coplanar waveguide (CPW) transmission lines fabricated using different conductor and dielectric materials. We characterize the nonlinear response of these devices by measuring the third-order intercept point (defined below) for transmission lines having different geometries. In order to understand the dependence of the observed third-order intercepts on transmission line length, we model the transmission line as a number of identical elements which are small enough that a lumped-element description is appropriate for individual elements. We assume a simple form for the third-order intercept of an individual segment and add the third-harmonic signals for a series of elements to obtain the third-

harmonic signal for the total structure. The analysis allows us to consider loss in the transmission line in the calculation of the third-order intercepts. These results for the transmission line of length L are then compared with measurements of third-order intercepts for coplanar waveguide lines of variable length fabricated from HTS superconductors (which can be considered to be lossless for the analysis presented here) and from ferroelectric materials (finite attenuation case). This analysis can provide valuable information about the nonlinear response of these technologically important materials. For the range of transmission line lengths considered here, this description of third-harmonic generation in distributed planar transmission lines works extremely well.

II. Calculation of third-order intercept point for a transmission line of length L

Our calculation of the third-order intercept for a series of N transmission line segments follows closely the discussion in [1] concerning the interconnection of weakly nonlinear components. We make many of the same assumptions, but we generalize the derivation in [1] to the case where the fundamental and the harmonic products of each segment do not have identical gain (or loss). This is an important generalization if we want to describe third-harmonic generation in transmission lines, for the attenuation of the third harmonic signal generated at frequency 3ω will in general be different from the attenuation at the fundamental frequency ω.

A. Definition of third-order intercept

We begin with an explicit definition for the third-order intercept. Experimentally, the third-order intercept is derived from measurements of the output fundamental (P_1) and third-harmonic (P_3) signals as a function of the incident power (P_{inc}). An example is shown in Fig. 1 for a CPW transmission line fabricated with a 170 nm layer of $Ba_{0.5}Sr_{0.5}TiO_3$ (BSTO). We describe the output fundamental signal vs. power with a line of slope 1 and intercept a :

$$\log P_1 = \log a + \log P_{inc} \ . \tag{1}$$

Similarly, the third harmonic is given by a line of slope three with intercept b:

$$\log P_3 = \log b + 3\log P_{inc} \ . \tag{2}$$

We write the third harmonic as a function of the output power P_1 in the fundamental:

$$\log P_3 = \log b + 3\left(\log P_1 - \log a\right) . \tag{3}$$

The third-order intercept point IP_3 is the value of the fundamental signal at which $\log P_1 = \log P_3$:

$$\log IP_3 = \log b + 3\left(\log IP_3 - \log a\right) . \tag{4}$$

The equation describing the third harmonic can now be written as

$$\log P_3 = -2\log IP_3 + 3\log P_1 \ . \tag{5}$$

The third-order intercept IP_3 defined in this manner is the output power in the fundamental (not the incident power at the device input) at the point where the fits to lines of slope 1 and slope 3 intersect in Fig. 1 (the units for power used from this point forward are decibels referenced to 1 mW, abbreviated dBm). This distinction between the output power in the fundamental and the incident power in the definition of IP_3 is important for structures with loss. Note that as used in (5), IP_3 is merely a parameter to desrcribe the intercept point for a line of slope 3 that is fit to the third-harmonic data. In real systems the third harmonic vs. power data deviates from a slope 3 well before P_3 becomes equal to P_1.

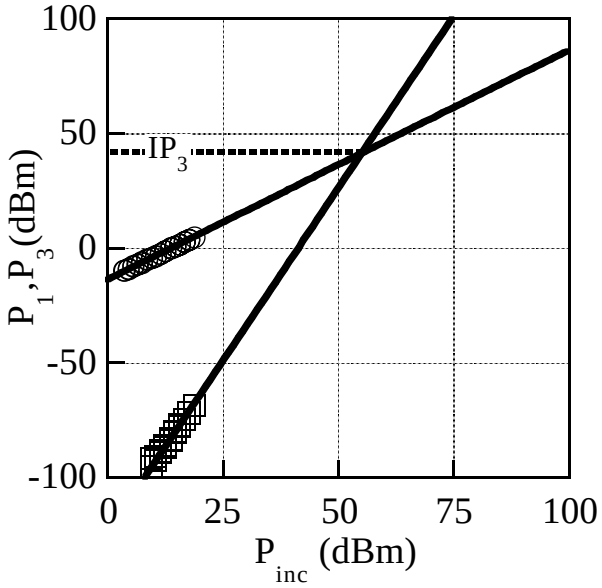

Fig. 1. Example of measured third-harmonic data for a CPW transmission line incorporating a 170 nm ferroelectric thin film ($Ba_{0.5}Sr_{0.5}TiO_3$). The third-order intercept IP_3 is determined by the intersection of fits to slope 1 and 3, to the fundamental and third harmonic, respectively.

B. Derivation of third-order intercept for transmission line with distributed nonlinearity.

We divide the transmission line of length L into a series of N small segments, each of length ℓ=L/N, as illustrated in Fig. 2. The number of segments N is large enough that each segment can be treated as a lumped element. Segment *m* generates a third-order signal $P_{3,m}$ and can be characterized by a third-order intercept $IP_{3,m}$. Each segment is also characterized by a voltage gain $G_m^{1/2}(\omega)$ which, for a transmission line of length ℓ, we take to be simply the propagation factor: $G^{1/2}(\omega) = e^{-\gamma(\omega)\ell}$ where $\gamma(\omega) = \alpha(\omega) + i\beta(\omega)$ is the complex propagation constant consisting of the attenuation constant $\alpha(\omega)$ and the phase constant $\beta(\omega)$. The gain factor will in general be different for the fundamental at frequency ω and the third harmonic at frequency 3ω: $G_m(\omega) \neq G_m(3\omega)$. We also assume that each segment is impedance matched to adjacent segments, and that the entire line is impedance-matched to the signal source and to the measurement system at the fundamental and third-harmonic frequencies.

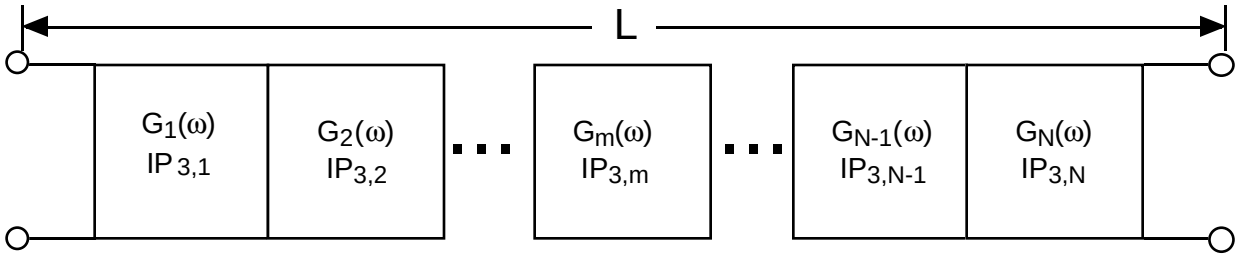

Fig. 2. Schematic diagram of transmission line of length L.

We begin by writing (5), which describes the third-harmonic signal, in linear form:

$$P_3 = \frac{P_1^3}{IP_3^2} . \qquad (6)$$

Solving for $1/IP_3$ gives

$$\frac{1}{IP_3} = \frac{P_3^{1/2}}{P_1^{3/2}}. \tag{7}$$

At the output of the last (nth) stage, the fundamental signal is given by

$$P_{1,N}^{1/2} = P_{1,inc}^{1/2}\left[G_1(\omega)G_2(\omega)\cdots G_N(\omega)\right]^{1/2}, \tag{8}$$

and the third-harmonic signal is given by the sum of third-harmonic signals generated by each element,

$$\begin{aligned} P_3^{1/2} = {} & P_{3,N}^{1/2} + P_{3,N-1}^{1/2} G_N^{1/2}(3\omega) + P_{3,N-2}^{1/2}\left[G_{N-1}(3\omega)G_N(3\omega)\right]^{1/2} \\ & + \cdots + P_{3,1}^{1/2}\left[G_2(3\omega)\cdots G_{N-1}(3\omega)G_N(3\omega)\right]^{1/2}. \end{aligned} \tag{9}$$

For a given segment m, the output power in the fundamental is given by

$$P_{1,m}^{1/2} = P_{1,inc}^{1/2}\left[G_1(\omega)G_2(\omega)\cdots G_m(\omega)\right]^{1/2}, \tag{10}$$

while the third-harmonic signal $P_{3,m}$ may be written as

$$P_{3,m}^{1/2} = \frac{P_{1,m}^{3/2}}{IP_{3,m}}. \tag{11}$$

Equation (11) applies only to segments whose third-harmonic response can be well described by a single value for $IP_{3,m}$. Substituting (10) into (11) for $P_{1,m}$ gives

$$P_{3,m}^{1/2} = \frac{P_{1,inc.}^{3/2}}{IP_{3,m}}\left[G_1(\omega)G_2(\omega)\cdots G_m(\omega)\right]^{3/2}. \tag{12}$$

Substituting (12) into (9) gives the third-harmonic signal generated by the total transmission line:

$$\begin{aligned} P_3^{1/2} = {} & IP_{3,N}^{-1} P_{1,inc}^{3/2}\left[G_1(\omega)G_2(\omega)\cdots G_N(\omega)\right]^{3/2} \\ & + IP_{3,N-1}^{-1} P_{1,inc}^{3/2}\left[G_1(\omega)G_2(\omega)\cdots G_{N-1}(\omega)\right]^{3/2}\left[G_N(3\omega)\right]^{1/2} \\ & + IP_{3,N-2}^{-1} P_{1,inc}^{3/2}\left[G_1(\omega)G_2(\omega)\cdots G_{N-2}(\omega)\right]^{3/2}\left[G_{N-1}(3\omega)G_N(3\omega)\right]^{1/2} \\ & + \cdots + IP_{3,2}^{-1} P_{1,inc}^{3/2}\left[G_1(\omega)G_2(\omega)\right]^{3/2}\left[G_3(3\omega)\cdots G_N(3\omega)\right]^{1/2} \\ & + IP_{3,1}^{-1} P_{1,inc}^{3/2}\left[G_1(\omega)\right]^{3/2}\left[G_2(3\omega)\cdots G_N(3\omega)\right]^{1/2}. \end{aligned} \tag{13}$$

Equation (13) represents the sum of third-harmonic signals generated by each element in the transmission line, taking into account explicitly the gain before and after each individual segment when $G_m(\omega) \neq G_m(3\omega)$.

We now use (8) to relate the incident power to the output power in the fundamental

$$P_{1,inc}^{3/2} = \frac{P_{1,N}^{3/2}}{\left[G_1(\omega)G_2(\omega)\cdots G_N(\omega)\right]^{3/2}} \ . \tag{14}$$

We substitute this expression into (13) to obtain

$$\begin{aligned} P_3^{1/2} = \ & \frac{P_{1,N}^{3/2}}{IP_{3,N}} + \frac{P_{1,N}^{3/2}}{IP_{3,N-1}} \frac{\left[G_N(3\omega)\right]^{1/2}}{\left[G_N(\omega)\right]^{3/2}} + \frac{P_{1,N}^{3/2}}{IP_{3,N-2}} \frac{\left[G_{N-1}(3\omega)G_N(3\omega)\right]^{1/2}}{\left[G_{N-1}(\omega)G_N(\omega)\right]^{3/2}} \\ & + \cdots + \frac{P_{1,N}^{3/2}}{IP_{3,2}} \frac{\left[G_3(3\omega)\cdots G_N(3\omega)\right]^{1/2}}{\left[G_3(\omega)\cdots G_N(\omega)\right]^{3/2}} + \frac{P_{1,N}^{3/2}}{IP_{3,1}} \frac{\left[G_2(3\omega)\cdots G_N(3\omega)\right]^{1/2}}{\left[G_2(\omega)\cdots G_N(\omega)\right]^{3/2}} \ . \end{aligned} \tag{15}$$

To calculate the third-order intercept for the entire structure, we use (7) to give

$$\frac{1}{IP_{3,tot}} = \frac{P_3^{1/2}}{P_1^{3/2}} \ . \tag{16}$$

Since P_1 in (16) is the output power in the fundamental, $P_1 = P_{1,N}$. Substituting (15) into (16) then gives

$$\begin{aligned} \frac{1}{IP_3} = \ & \frac{1}{IP_{3,N}} + \frac{1}{IP_{3,N-1}} \frac{\left[G_N(3\omega)\right]^{1/2}}{\left[G_N(\omega)\right]^{3/2}} + \frac{1}{IP_{3,N-2}} \frac{\left[G_{N-1}(3\omega)G_N(3\omega)\right]^{1/2}}{\left[G_{N-1}(\omega)G_N(\omega)\right]^{3/2}} \\ & + \cdots + \frac{1}{IP_{3,2}} \frac{\left[G_3(3\omega)\cdots G_N(3\omega)\right]^{1/2}}{\left[G_3(\omega)\cdots G_N(\omega)\right]^{3/2}} + \frac{1}{IP_{3,1}} \frac{\left[G_2(3\omega)\cdots G_N(3\omega)\right]^{1/2}}{\left[G_2(\omega)\cdots G_N(\omega)\right]^{3/2}} \ . \end{aligned} \tag{17}$$

For the special case where $G_m(3\omega) = G_m(\omega)$, (17) is equivalent to (4.1.49) with n=3 in [1].

C. Third-order intercept for transmission line with identical elements

If we assume that all the elements in the transmission line are identical, then $IP_{3,m} = IP_{3,m'}$ and $G_m = G_{m'}$ for all m and m´, and (17) can be written as

$$\frac{1}{IP_{3,tot}} = \frac{1}{IP_{3,m}} \sum_{i=0}^{N-1} \left[\frac{G_m^{1/2}(3\omega)}{G_m^{3/2}(\omega)} \right]^i . \tag{18}$$

Here $IP_{3,m}$ is the third-order intercept and G_m is the gain of an individual segment.

Equation (18) is an expression for the total third-order intercept for a transmission line consisting of N identical elements, each of which can be described by a third-order intercept point

$IP_{3,m}$. This expression is significant for two reasons: it allows us to use simple lumped-element expressions for $IP_{3,m}$ (which are derived below for two examples), and it allows us to take into account losses and phase effects in transmission lines in a simple manner.

D. Limitations of this approach

We have derived the expression (18) for the third-order intercept for the case of a weakly nonlinear transmission line of arbitrary length. To arrive at this expression, we have assumed that the nonlinear effects of individual elements are small and that individual segments do not interact. This is equivalent to saying that each transmission line segment transmits the incident fundamental and third-harmonic signals as though it were a linear element. The only effect of the nonlinearity is to generate some additional third-harmonic signal due to the element itself. This derivation will be expected to break down for elements where the nonlinear effects are sufficiently large. In practice this limits this analysis to the case where the third-harmonic signal is much smaller than the fundamental: that is, when $P_3 << P_1$. This limitation does not present a problem for defining the third-order intercept point IP_3 for our data, because IP_3 is used simply to describe the intercept point for a line of slope 3 fit to our data, and does not require $P_3 \sim P_1$.

III. Application to planar transmission lines

In order to apply the expression (18) for $IP_{3,tot}$ to our experimentally obtained values of $IP_{3,meas}$, we need to obtain a suitable expression for the third-harmonic signal generated by an individual transmission line segment ($IP_{3,m}$). We will assume for the devices examined here that the third-harmonic signal is generated by either a nonlinear inductance, which is used to describe the HTS transmission lines, or a nonlinear capacitance, which is used to describe the ferroelectric transmission lines. We then use a simple lumped-element model to describe the third-order intercept of an individual segment.

A. Lumped-Element Models for IP_3

For a nonlinear inductor, we use the following form for the inductance per unit length

$$L(I) = L_0 + L' I^2, \tag{19}$$

where L_0 is the linear inductance per unit length. Such an expression has been used by Dahm et al. to describe nonlinear effects in (lumped-element) HTS resonators [2]. We use the nonlinear inductance described by (19) to calculate third-harmonic generation in a section of transmission line. We assume that the nonlinear term in the inductance generates a third-harmonic signal, but does not appreciably affect the linear properties of the transmission line.

To determine the effect of the nonlinear inductance in (19) on the measured response of our circuit, we follow [3] and calculate the voltage generated by a (lumped-element) nonlinear inductor of length ℓ:

$$V(t) = \ell L(I)\frac{dI}{dt} = \ell L_0 \frac{dI}{dt} + \ell L' I^2 \frac{dI}{dt} \ . \tag{20}$$

We assume that the inductor length ℓ is small enough compared to a wavelength that the lumped-element approach is valid. We assume a single-tone input signal at an angular frequency ω:

$$I(t) = I_0 \cos(\omega t). \tag{21}$$

Substituting (21) into (20) produces a voltage signal at frequency 3ω:

$$V(3\omega) = \frac{\ell L' \omega I_0^3}{4} \sin(3\omega t) \ . \tag{22}$$

We now calculate the power in the third harmonic for a section of transmission line of characteristic impedance Z_0:

$$\begin{aligned} P_3 &= \frac{1}{2Z_0}|V_3|^2 \\ &= \left[\frac{\omega L' \ell}{4}\right]^2 \frac{I_0^6}{2Z_0} \quad = \quad \left[\frac{\omega L' \ell}{2Z_0^2}\right]^2 \frac{I_0^6 Z_0^3}{8} \quad . \end{aligned} \tag{23}$$

In this treatment we consider only the third-harmonic signal traveling in the forward direction. Using the expression for the power in the fundamental $P_1=I_0^2 Z_0/2$ we obtain for P_3 in decibels

$$P_3 = 2*10\log_{10}\left(\frac{\omega L' \ell}{2Z_0^2}\right) + 3*10\log_{10}(P_1) \ . \tag{24}$$

In (24) we have neglected the attenuation of the individual segment, and we have made the assumption that the impedance of the measurement system is matched to the characteristic impedance Z_0. If we plot the power in the third harmonic vs. P_1, we obtain a line of slope 3 with an intercept given by the first term in (24). For a line of slope 3 with an intercept b, the third-order intercept is simply $IP_3 = -b/2$. Using this expression, we obtain for the third-order intercept for a line of length ℓ (in linear units):

$$IP_{3,\ell} = \frac{2Z_0^2}{\omega L' \ell} \ . \tag{25}$$

We follow a similar derivation for the nonlinear capacitor, assuming the following form for the nonlinear capacitance per unit length:

$$C(V) = C_0 + C' V^2 . \tag{26}$$

We then obtain for the third-order intercept of a line of length ℓ

$$IP_{3,\ell} = \frac{2}{\omega C' \ell Z_0^2} . \tag{27}$$

Once we have obtained expressions for the third-order intercepts for a single transmission line element of length ℓ = L/N, we combine all N segments using (18). For both the nonlinear inductance and nonlinear capacitance, we obtain expressions of the form

$$IP_{3,tot}^{-1} = IP_{3,L/N}^{-1} \sum_{i=0}^{N-1} \left[\frac{G_m^{1/2}(3\omega)}{G_m^{3/2}(\omega)} \right]^i$$
$$= IP_{3,L}^{-1} \left\{ \frac{1}{N} \sum_{i=0}^{N-1} \left[\frac{G_m^{1/2}(3\omega)}{G_m^{3/2}(\omega)} \right]^i \right\} \quad , \tag{28}$$

where $IP_{3,L}$ is the appropriate lumped-element expression for a transmission line segment of length $\ell = L$. In writing (28), we have used the fact that $IP_{3,L/N} = N \cdot IP_{3,L}$, which is apparent from (25) or (27). Equation (28) says that the third-order intercept for the total structure is simply the lumped-element expression for the third-order intercept point for a line of length L multiplied by a numerical factor that depends on the transmission line gain factors.

B. Comparison to Experimental Data for HTS Transmission Lines

For superconducting transmission lines, we assume that the attenuation constant can be neglected ($\alpha = 0$). This gives for the propagation constant $\gamma = i\beta$ where $\beta = \omega/v_{phase}$ is the phase constant at frequency ω corresponding to a phase velocity v_{phase}. The gain factor for a transmission line of length ℓ at the fundamental and third-harmonic frequencies is then $G_m^{1/2}(\omega) = e^{i\beta\ell}$ and $G_m^{1/2}(3\omega) = e^{i3\beta\ell}$. For this case, the gain factors in (28) cancel; we obtain $IP_{3,tot} = IP_{3,L}$. The resulting fit of the measured third-order intercepts to the length dependence of the lumped-element model given in (25) is shown in Fig. 3 for several different center conductor linewidths. We find excellent experimental confirmation of the lumped-element behavior from measurements of our HTS transmission lines, even when the transmission line length approaches an appreciable fraction of the effective wavelength (for the data shown in Fig. 3, the effective wavelength is estimated to be 28 mm). This analysis means that we can use the lumped-element description to characterize superconducting transmission lines that have lengths approaching the effective wavelength. The parameter L´ extracted from this analysis can be used to obtain physical information about the HTS material. From the value of L´ extracted from the data shown in Fig. 3, we can calculate the dependence of the superconducting penetration depth on the applied current density [4]. We obtain consistent values for this quantity for all three linewidth structures shown in Fig. 3.

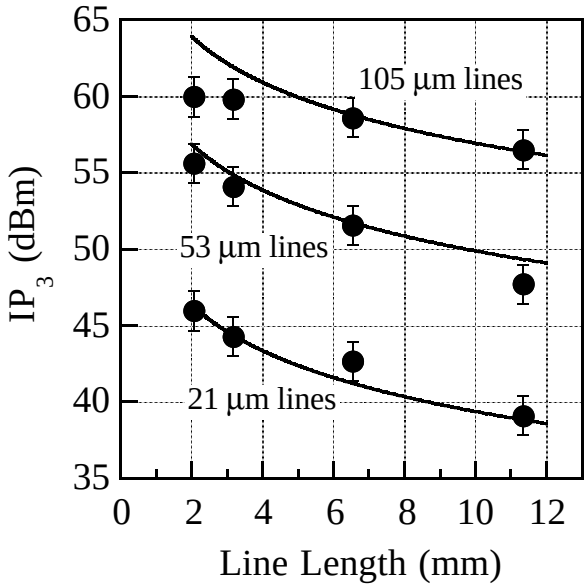

Fig. 3. Third-order intercepts vs. line length for an HTS transmission line with a 5 GHz fundamental signal. The center conductor linewidths are 21 μm, 53 μm, and 105 μm. The solid lines are a fit to a lumped-element model.

C. Comparison to Experimental Data for Ferroelectric Transmission Lines

The attenuation of ferroelectric transmission lines is significant and cannot be ignored in our analysis. We measure the attenuation per unit length for a set of CPW transmission lines incorporating a BSTO thin film using on-wafer calibration techniques [5], which is shown in Fig. 4. We then use the measured attenuation constants at the fundamental [$\alpha(\omega)$] and the third harmonic [$\alpha(3\omega)$] frequencies to calculate $IP_{3,tot}$ in (28). For a segment of length $\ell = L/N$ we obtain $G_m^{1/2}(\omega) = \exp[-\alpha(\omega)L/N]\cdot\exp[i\beta\ell]$ and $G_m^{1/2}(3\omega) = \exp[-\alpha(3\omega)L/N]\cdot\exp[i3\beta\ell]$, with $\beta = \omega/v_{phase}$ as before. Substituting into (28) gives

$$IP_{3,tot}^{-1} = IP_{3,L}^{-1}\left\{\frac{1}{N}\sum_{i=0}^{N-1}\left[\frac{e^{-\alpha(3\omega)L}}{e^{-3\alpha(\omega)L}}\right]^{i/N}\right\}. \qquad (29)$$

The phase constants cancel out in (29) in the same manner as for the superconducting case. However, unlike the superconducting case, the attenuation constant is significant and cannot be neglected.

In practice we allow N to become large and perform the summation in (29) numerically. We then obtain an expression of the form $IP_{3,tot} = IP_{3,L}/K(L)$, where $K(L)$ is the numerical factor represented in braces in (28), which depends on the transmission line length and attenuation constant. We plot in Fig. 5 the measured third-order intercepts for our ferroelectric transmission lines as a function of line length. We also plot in Fig. 5 a fit to the length dependence of the bare lumped-element model given in (27), and the transmission line model that includes the attenuation, given in (29). Clearly the modification of the lumped-element model represented by (29) describes the data much better than the bare lumped-element model. The values obtained from this analysis for the parameter C´ can subsequently be used to evaluate the voltage tunability of a given ferroelectric material or structure. This is an important parameter to optimize for applications that are interested in voltage tunable devices.

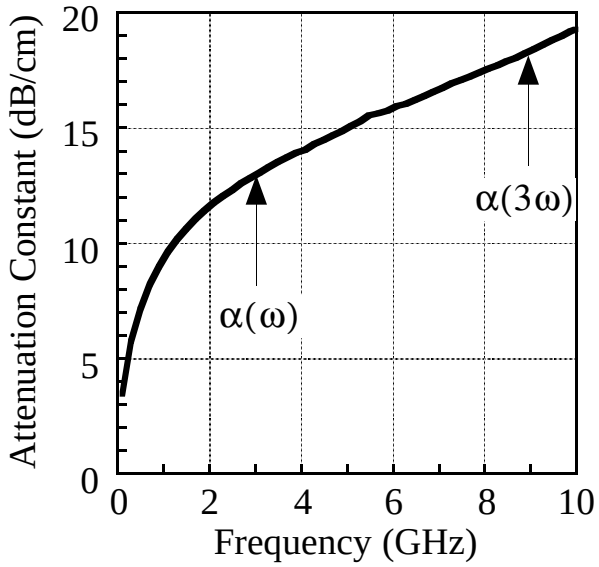

Fig. 4. Measured attenuation constant vs. frequency for $Ba_{0.5}Sr_{0.5}TiO_3$ loaded CPW transmission lines. The center conductor linewidth is 10 μm.

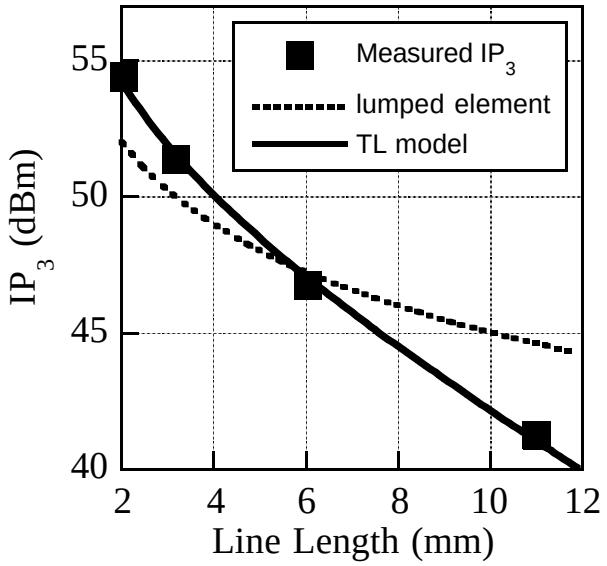

Fig.5. Third-order intercepts vs. line length for a ferroelectric transmission line with a 3 GHz fundamental signal. The filled symbols are IP_3 extracted from the measured data. The dashed line is a fit to the length dependence of the lumped-element model alone, while the solid line is the lumped-element fit corrected for transmission line attenuation according to (29).

IV. Conclusions

We calculate the third-order intercept of transmission lines incorporating a distributed nonlinear inductance or capacitance. This analysis allows us to use simple lumped-element models to understand nonlinear effects in transmission lines, even for line lengths on the order of, or greater than, the effective wavelength. We can understand the effect of arbitrary transmission line length for lines both with and without losses, provided that the third-harmonic signal remains small. This analysis can be used to extract useful information from nonlinear measurements of both HTS and ferroelectric materials.

V. Acknowledgements

We would like to acknowledge I. Takeuchi, H. Chang, and X.-D. Xiang of Lawrence Berkeley National Laboratory for supplying the BSTO sample. This work was supported in part by the Office of Naval Research. The contribution of J.C.B. was supported by a NIST/NRC postdoctoral research associateship.

VI. References

[1] S. A. Maas, *Nonlinear Microwave Circuits* (Artech House, Boston, 1988), pp. 170-172.
[2] B.A. Willemsen, K.E. Kihlstrom, T. Dahm, D.J. Scalapino, B. Gowe, D.A. Bonn, and W.N. Hardy, "Microwave loss and intermodulation in $Tl_2Ba_2CaCu_2O_y$ thin films," Phys. Rev. B Vol. 58, 1998, pp. 6650-6654.
[3] R.B. Hammond, E.R. Soars, B.A. Willemsen, T. Dahm, D.J. Scalapino, and J.R. Schrieffer, "Intrinsic limits on the Q and intermodulation of low power high temperature superconducting microstrip resonators," J. Appl. Phys. Vol. 84, 1998, pp. 5662-5667.
[4] James C. Booth, J.A. Beall, D.A. Rudman, L.R. Vale, and R.H. Ono, "Geometry dependence of nonlinear effects in high temperature superconducting transmission lines at microwave frequencies," submitted to J. Appl. Phys.
[5] R.B. Marks, "A multiline method of network analyzer calibration," IEEE Trans. Microwave Theory Tech. Vol. 39, 1991, pp. 1205-1215.